MECHANIKA TEORETYCZNA
I STOSOWANA
Journal of Theoretical
and Applied Mechanics
4, 35, 1997

IDENTIFICATION OF THE ROTOR BLADE WAKE AND 3D TURBULENCE STRUCTURE IN AXIAL FLOW LOW SPEED COMPRESSOR STAGE

ANDRZEJ S. WITKOWSKI

TADEUSZ J. CHMIELNIAK

MICHAŁ D. STROZIK

Institute of Power Machinery, Silesian Technical University, Gliwice

e-mail: root@zcmp.imiue.gliwice.edu.pl

The main objective of these investigations is to provide study of the turbulence structure in the wake mixing region of the axial flow low speed compressor rotor exit. The unsteady flow under two different operating conditions has been investigated by means of periodic multisampling with the use of straight and 90 degree triple-split fiber probes to find out the influence of aerodynamic compressor load on threedimensional turbulent flow field. Tip clearance effects, secondary flow near the hub and outer wall and radial flow in the wake, turbulence intensity and Reynolds stresses and, also, the decay of the rotor wakes can be obtained using this method.

Key words: axial low speed compressor stage, turbulence intensity, periodic multisampling

Nomenclature

A, B	–	calibration coefficients for triple-split probe
C	–	velocity, absolute frame
E	–	anemometer voltage
M	–	number of sampled points
N	–	number of revolutions
P_0	–	stagnation pressure
r	–	radius
T	–	turbulence intensity

U – peripheral velocity
W – velocity, relative frame
α – flow angle in the circumferential direction, absotule frame
β – flow angle in the circumferential direction, relative frame
θ – angular distance from the stagnation point of triple-split probe
ψ – mass averaged pressure rise coefficient, $\psi = (p_{02} - p_{01})/(0.5U_T^2)$
φ_T – tip averaged flow coefficient, $\varphi_T = \bar{c}_z/U_T$

Subscripts and superscripts

1,2 – rotor inlet and exit plane, respectively
r, z – radial and axial direction, respectively
T – at the tip radius
ϑ – circumferential direction
$\widetilde{(\cdot)}$ – ensemble averaged
$\overline{(\cdot)}$ – mean value

1. Introduction

Understanding of the flow physical effects associated with the wake/boundary layer interaction, relative motion of the rotor and stator pressure fields and unsteady separation, trailing edge vortex shedding, transition and random turbulence fluctuation, etc., in the turbomachinery and capability of the computer codes to predict its effects on the blade row performance are essential for eventual including unsteady effects into the design process. The unsteady transition, resulting mainly from high turbulence intensity in the wake has been found as changing significantly the profile loss (Hodson, 1990). The influence of wake disturbed inlet flow on the overall performance of a compressor stator row was investigated in detail by Schulz (1990). The literature available on the influence of different operating conditions on the structure of turbulence in axial flow compressor stage downstream of the rotor is very limited. Evans (1975) published extensive measurement results of the turbulence and unsteadiness level downstream of an axial-flow compressor rotor at different values of flow coefficient but at the mid-span position only. Besides, the measurements taken in this paper are based on the assumption that the radial velocity is zero. The turbulence properties at the compressor rotor exit, measured with stationary three sensors, hot wire probe, are reported by Davino and Lakshminarayana (1982) but for one operating point only. Lately,

Camp and Shin (1995) have described the measurement and processing of turbulence data from three low-speed, four stage compressor rigs. Their results show how the values of turbulence intensity and length scale at the midspan change with: position in the blade passage, flow coefficient and the value of the design stage loading coefficient. They did not considered the detailed flow structure. The objective of the present study is to investigate the characteristic flow parameters which govern the unsteady flow field in the blade row spacing and stator passage of the low speed axial flow compressor stage under two different operating conditions.

2. Axial-flow compressor facility

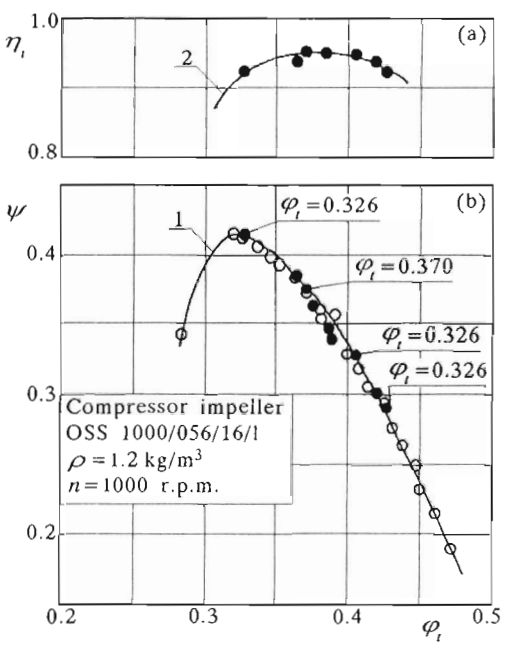

Fig. 1. Overall performance characteristics of the rotor

The axial-flow compressor facility used in this investigation is described in detail in other papers (Witkowski et al. 1994, 1996). The dimensionless overall performance characteristics of the rotor are shown in Fig. 1. In the present paper only the results for normal ($\psi_T = 0.374$) and higher than normal

(φ_T = 0.426) flow coefficients are presented. The hub/annulus-wall diameter ratio of the compressor rotor is 0.56, with the diameter of the annulus wall equal to 1.0 m. The rotor consists of 16 cambered and twisted blades of British C-4 section, designed for free-vortex operation. It is followed by a 13-blade stator row, again of free-vortex type. The outflow curvilinear diffusor with the throttling blades which provides control of the stage operation characteristics is placed downstream the stator. The compressor stage is set on the suction side of the measuring collector. The research consists of mass flow measurements through an aerodynamically designed inlet nozzle. A 30 kW direct current motor mounted in the cradle and allowing for continuous speed variation up to 3000 r.p.m. was used.

3. Probe, instrumentation, and data transmission system

The flow fields upstream and downstream of the rotor have been sampled periodically using both straight and 90 degree triple-split fiber probes, respectively, similar to that used by Witkowski et al. (1994, 1996). The 3-sensor probe was built of three films-sensor placed in a parallel path, 120 degree displaced, on a common quartz fiber. The working principle of the triple-split fiber probes is based on variation in the local heat transfer on cylinders in a crossflow. The probe calibration was performed employing a low turbulence open-jet calibration facility. The resulting calibration was corrected for yaw and pitch angle sensitivity, and temperature variation. A more detailed description of the triple-split fiber probes and their calibration procedure is given by Jørgensen (1982), Witkowski et al. (1994). The stationary probe measurement technique employed was developed by Witkowski et al. (1994), and has been continuously improved to increase the accuracy. An optical shaft encoder provided a pulse for every 0.1 degree of impeller rotation. This was used to trigger a simultaneous sampling of the three anemometer voltages digitised in the measured module which consists of three paralell working sample hold amplifiers, an analog multiplexer and a 12 bit analog digital converter. The Analog Digital converter used a sampling frequency of up to 100 kHz. It allowed for simultaneous processing of three anemometer signals with a minimum period of 31.5 ms. Ensemble averaging was the main data reduction method used in the experiments. It is particularly suitable for investigation of the periodically unsteady flow process, enabling separation of periodic fluctuations from the random ones (Bendat and Piersol, 1986; Binder et al., 1989). This procedure has already been used frequently in hot-wire probe and LDV-measurements

in investigations of unsteady flows in turbomachinery (Lakshminarayana and Poncet, 1974; Davino and Lakshminarayana, 1982; Shultz, 1989; Gallus et al., 1991). Various mean and turbulent flow characteristics in absolute frame of reference were obtained statistically with instantaneous velocities. A detailed discussion of the data processing procedure is given by Witkowski et al. (1996).

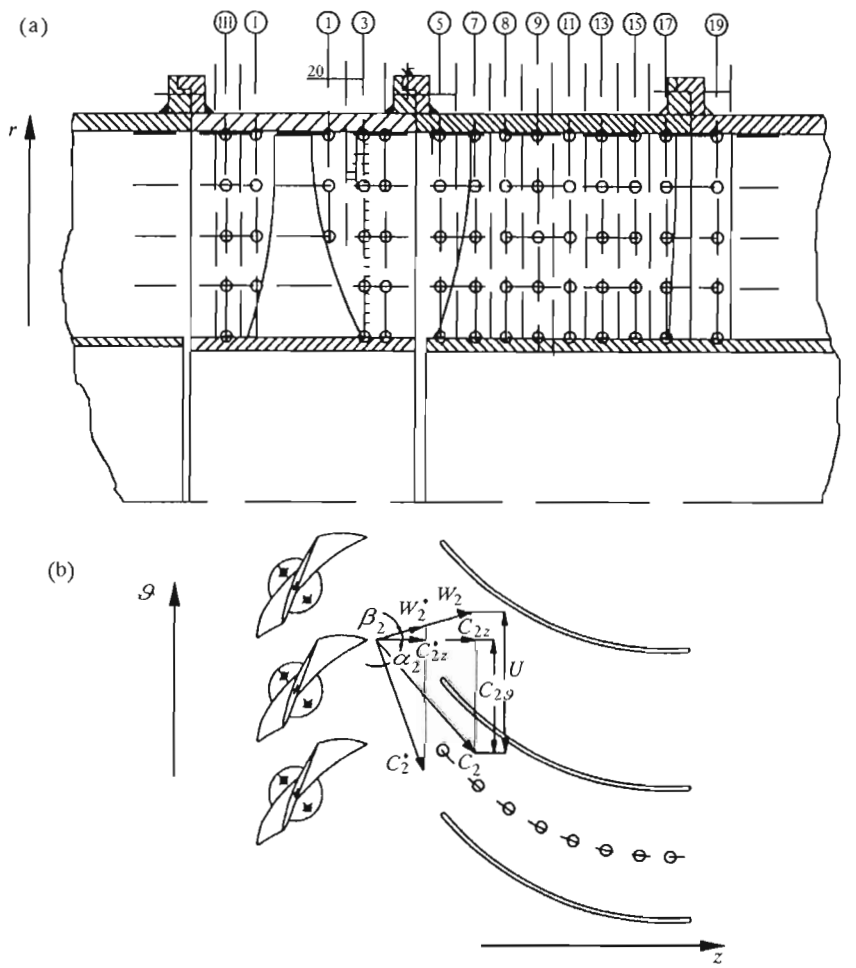

Fig. 2. Locations of measurements

4. Test programme

The objective of the investigation reported in this paper was to determine:

- The influence of aerodynamic compressor load on the rotor blade wake geometry and on the turbulence intensity and turbulence correlations at location 3 (Fig.2)
- The rotor blade wake decay at selected axial locations downstream of the rotor and on the centerline of the stator passage (Fig.2)
- The spanwise characteristics of unsteady flow at selected axial positions
- Secondary flow field plots.

5. Identification of the rotor blade wake geometry

The presented method was at first applied to measurements of the flow field at two flow coefficients ($\varphi_T = 0.374$, and $\varphi_T = 0.432$) for the middle radius, 50 mm downstream of an axial flow rotating blade with the use of straight and 90 degree versions of the triple-split fiber probe. A sequence of 100 real-time samples of velocities were recorded over roughly two blade passing periods and averaged over 1000 revolutions. Fig.3 shows typical results of the ensemble-averaged mean components of velocity for two different flow coefficients. It should be emphasised here that the most interesting information about the rotor flow can be obtained from the analysis of outlet relative velocity W distribution. It makes it possible to identify the exact geometry of rotor blade wake. The region of sudden decrease in the axial component of absolute velocity and in the relative velocity indicates the blade wake, the left side of which corresponds to the pressure side and the other one to the suction side. Thus it is possible to find the values of profile boundary layer thickness. Fig.3 shows that the pressure surface boundary layer is slightly thicker than that on the suction surface. It seems to be the result of low aerodynamic load of the rotor at the analysed operating points. A typical result of axial and tangential velocity is also shown in Fig.3. The axial velocity shows a defect in velocity as each wake passes the probe, while the tangential velocity shows a peak, in phase with the axial velocity defect. While the axial and tangential components of velocity profiles are nearly symmetrical about the wake center,

the profile of radial component of velocity is strongly asymmetrical. Asymmetry in the radial velocity component results from the imbalance between centrifugal and pressure forces in the wake area. The flow is subjected to complex interaction resulting from the rotor blade boundary layer, the rotor blade wake and the secondary flow. It causes the radial component to increase continuously in the free stream between suction side of the rotor blade wake and pressure side of the successive wake in the circumferential direction, than it decreases strongly in the wake region. So the radial component of absolute velocity attains the peak on the pressure side and the lowest value on the suction side of the blade wake.

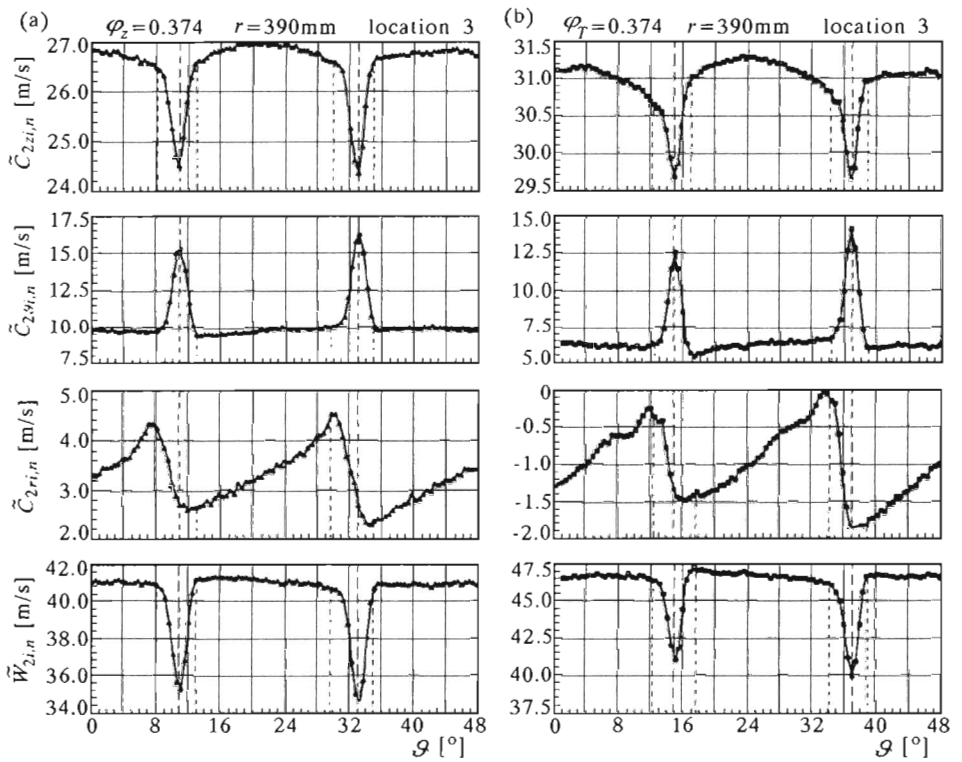

Fig. 3. Ensemble averaged absolute and relative velocity components for two operating points

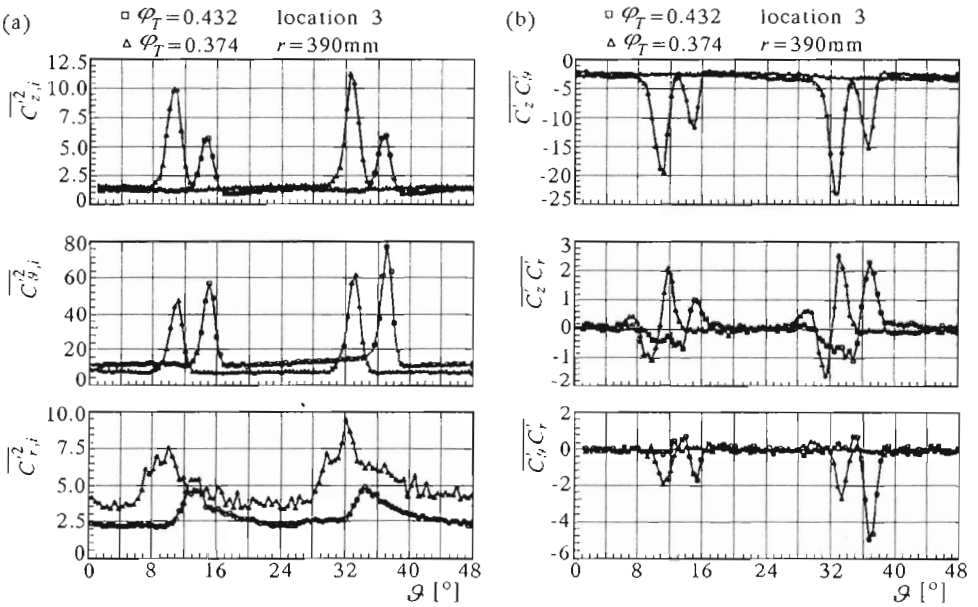

Fig. 4. Comparison between the Reynolds stresses for two operating points at the midspan location

6. Turbulent shear stress profiles at the midspan location

The unsteady flow in a low pressure single axial flow compressor stage for two different operating conditions was investigated to determine the influence of the compressor load on the velocity fluctuations. Fig.4 illustrates the comparison the distributions of six Reynolds stresses for two different operating conditions at the midspan location. To calculate the Reynods stresses three components of the fluctuating velocity are taken: as, C'_z in the axial direction, C'_ϑ perpendicular to that velocity and C'_r in the radial direction. The distributions of stresses are consistent with the velocity gradients in terms of the turbulent shear flow equations. In both cases of flow coefficients, the turbulent stresses in the rotor exit-flow are very small in the free stream and increase in magnitude near the wake center. At this location they reach their maximum value. Whilst the axial and tangential stresses have nearly symmetrical profiles about the wake center the radial stresses exibit an asymmetric profile. Radial stresses increase continuously in the circumferential direction and attain the peak on the pressure side of the wake. This observation indicates the effect of secondary flows on the radial stresses.

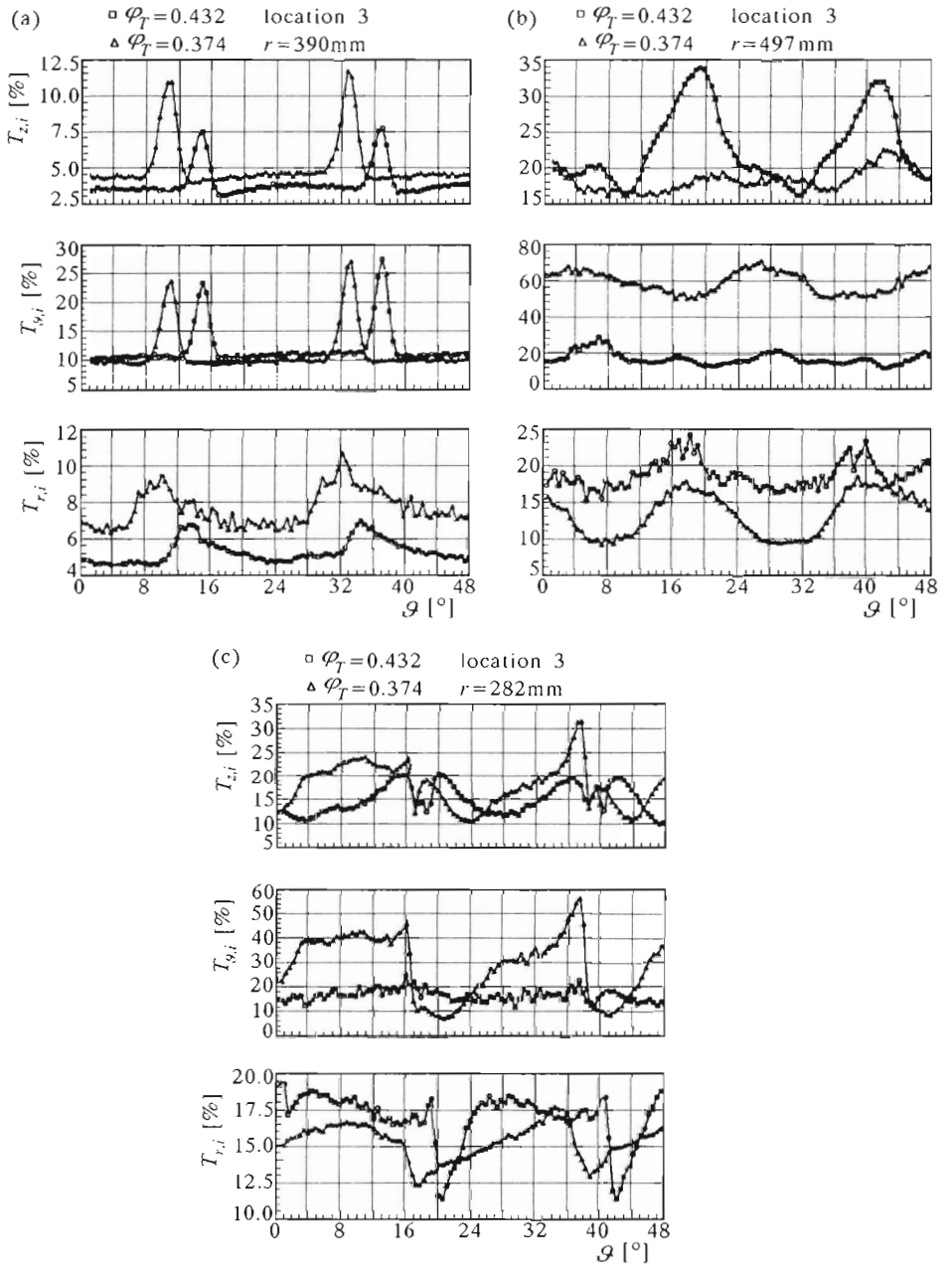

Fig. 5. Comparison between turbulence intensities for two operating points and at three radii

7. Turbulence intensity profiles

The comparison between the tangential variations of the three turbulent intensity components at three radii for two different operating conditions is shown in Fig.5. The three components of turbulent intensity and six Reynolds stresses, for the middle radius, show the wake structure. In all three cases the turbulent intensities increase rapidly close to the rotor wake and attain the peak near the wake center line. High turbulence intensities in the wake region indicate that the areas of mixing the pressure and suction side profile boundary layers are a highly active centers of turbulence. This can also be seen by a dramatic increase in the turbulence correlation (Fig.4). Fig.4 and Fig.5 also show that the turbulence correlation and turbulence intensity plots at position 3, for the middle radius, account for nearly isotropic turbulence outside the wake, and anisotropic turbulence in the wake region. For the middle radius of the rotor blade the turbulence production is generally higher at the nominal point of operation. The authors speculate that this may have been caused by a higher aerodynamic load of the rotor blades at the analysed point of operation. A comparison between turbulent components intensity levels, shows that the axial and radial components of intensity are approximately equal in the wake region. The tangential intensities are generally higher than the axial and radial ones. This results from the strong effects of blades rotation on the downstream tangential turbulence. Whilst the axial and tangential intensity profiles are nearly symmetrical, the radial components of turbulence intensity profiles are clearly asymmetrical. The asymmetry observed in the radial profiles results from the differential growth of turbulence on the suction and pressure surfaces of the rotor blade. Considerable increase of all three components of turbulence intensity, for the both operating point, i.e., at the hub and in the tip region of the rotor blade can be observed. This is due to higher disturbances of the flow which is subjected to complex interaction resulting from annulus-wall boundary layer, rotor wake, tip leakage flow, and secondary flow, respectively. For the normal operating point, the component of tangential turbulent intensity in the leakage-flow mixing region is found to be much higher than the corresponding axial and radial components. But for a higher value of the flow coefficient the relations are different. High value of tangential turbulence intensity in the tip region, at the nominal point of operation may be due to higher magnitude of aerodynamic load, providing an increase in the leakage flow. The tendency of the latter results is different from that reported by Davino and Lakshminarayana (1982).

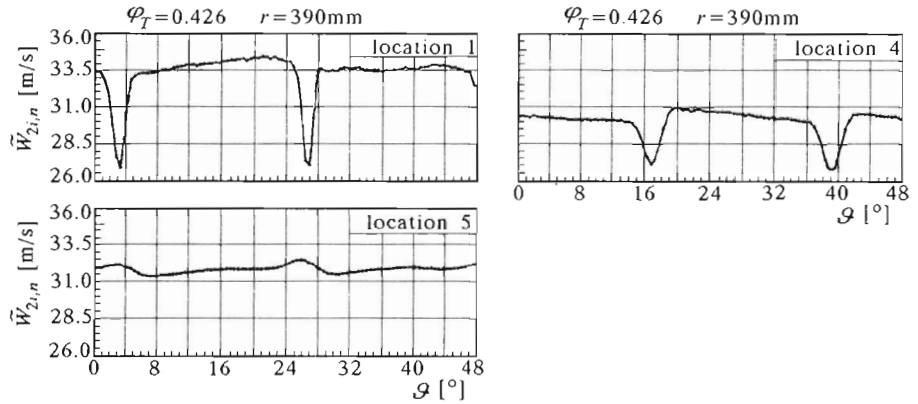

Fig. 6. Wake decay in the relative flow

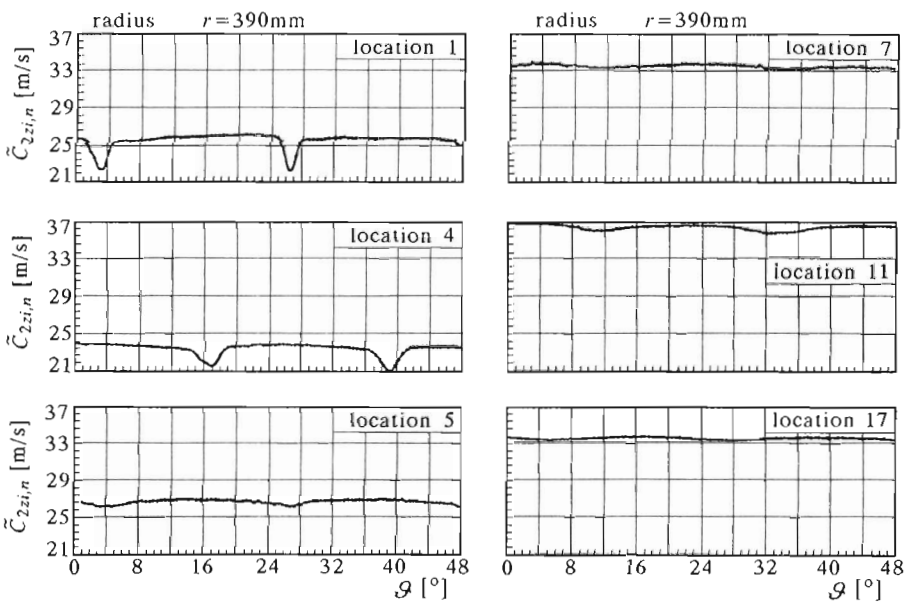

Fig. 7. Wake decay in the absolute flow

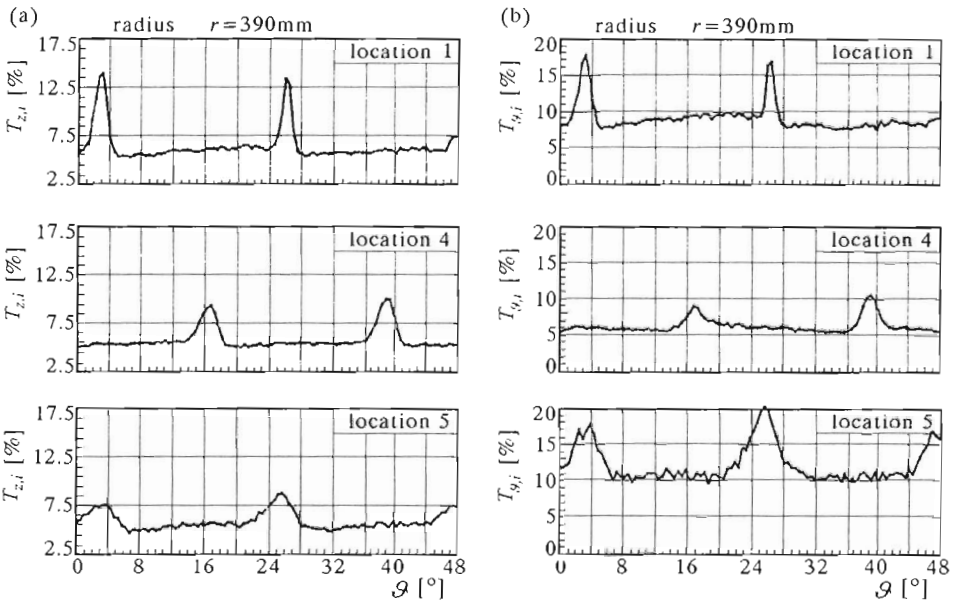

Fig. 8. Decay of axial and tangential components of the turbulence intensity

8. Decay characteristics of velocity and turbulence

In order to get a basic understanding of the wake decay dependence on the axial distance downstream of the rotor, the unsteady flow was determined at selected axial locations, and initially on the middle radius. Fig.6 to Fig.8 show that the rotor blade wake and components of turbulence intensity are slightly asymmetrical at location 1 but tend to become symmetrical far downstream. The asymmetry in the profiles seems to result from the differential growth of turbulence on the suction and pressure surface of the rotor blade. At location 5, just upstream of the back stator vane, the relative (Fig.6) and absolute (Fig.7) defect of the rotor wake is significantly decreased. This indicates that the axial distance between the rotor trailing edge and the stator leading edge, which is 1.15 rotor chord lengths at midspan, is chosen properly. Hodson (1983), and Schultz (1989) reported strong influence of the rotor-wake on incidence of the downstream stator. High incidence results in big profile losses, and consequently, affects the stage performance. It is clear that the incidence to the stator would be unacceptably high if the rotor-stator spacing

was too close. The second step, the wake decay was also determined along the centerline of the stator blades in the absolute frame of references. The wakes were found to have been further continuously smoothed in the presence of the stator. The absolute velocity wake depth (Fig.7) decreased 90% from 4 m/s at location 1 just downstream the trailing edge of the impeller blade to 4 m/s at location 17. The decrease in the rotor blade wake is reflected in lower velocity gradients normal to the wake. Therefore the components of turbulence production in the wake (Fig.8) decrease in the downstream location of the rotor due to the mixing effects. There are significant differences in the decay characteristics of the axial and tangential components of the wake of velocity, turbulence intensities and turbulence correlation between the blade rows. While the axial components of turbulence intensity decrease continuously in the rotor-stator blade row spacing (Fig.8a), the tangential components of the turbulent intensity and turbulent correlation strongly increase on the plane just upstream the inlet edges of the stator blades as a result of their backward reaction (Fig.8b). It increases also the level of tangential turbulence and turbulence correlation inside the stator blade passage in comparison with the axial turbulence.

9. Spanwise characteristics of unsteady flow

In order to get the spanwise characteristics of unsteady flow 39 radial measurements were taken just downstream (location 3) of the blade rotor (Fig.2). The measured exit velocity distribution in the relative frame, for higher than the nominal flow coefficient is shown in Fig.9a. The wake can be clearly distinguished by reduced velocity and increased turbulence (Fig.9b). The width of the rotor wake is affected not only by the state of the profile boundary layer, but mainly by a complex secondary flow and mixing phenomena. For more detailed analysis of the flow structure in the spanwise directions, Fig.10 shows the comparison between the turbulence intensities at the three radii (hub, mid radius, and outer wall) for two different operating conditions. Near the tip of the rotor, the flow pattern is very complex. The leakage flow, mixing of pressure and suction side profile boundary layers, horseshoe vortex and irregular shed van Karman vortices are superimposed. So those phenomena strongly influence the exit velocity distribution and caused significantly higher turbulence in that region.

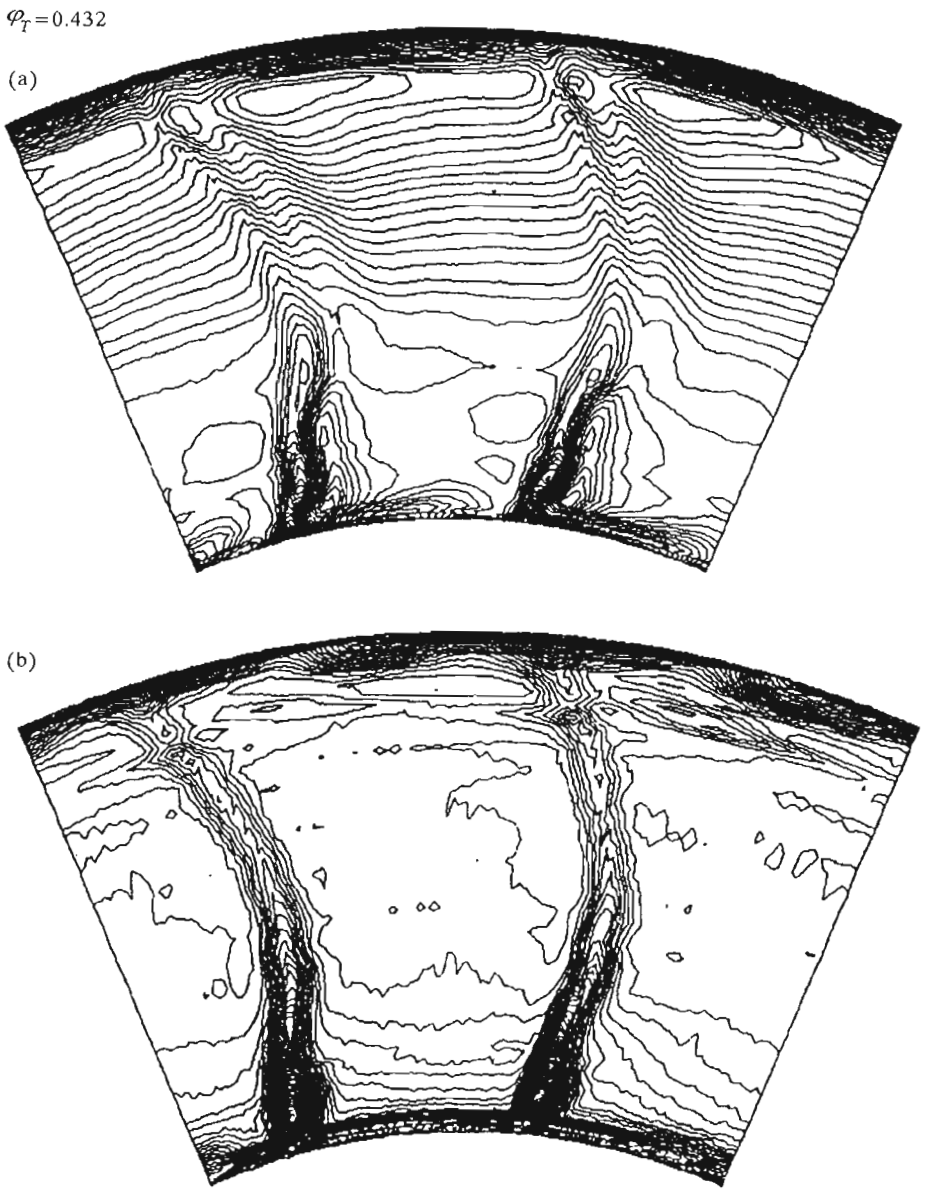

Fig. 9. Absolute velocity (a) and turbulence (b) contour plots downstream of the rotor

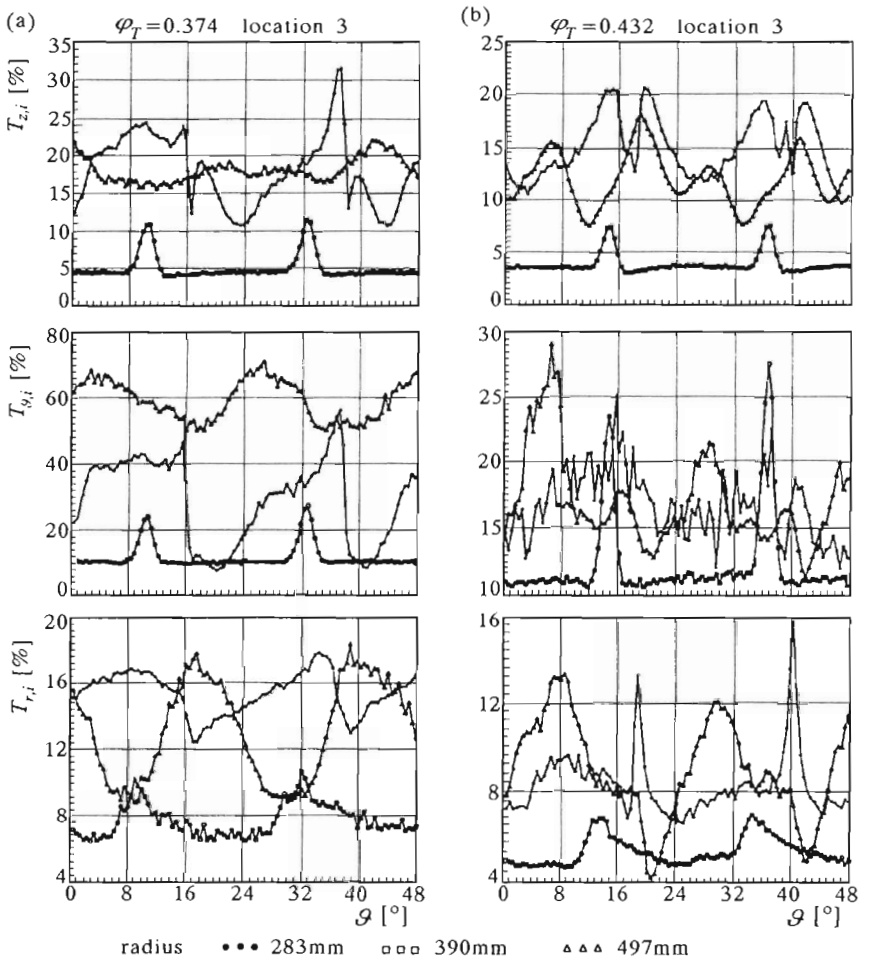

Fig. 10. Distributions of the turbulence intensities at the exit of the rotor row

10. Secondary flow

In Fig.11 the secondary flows in the absolute frame of reference for two different operating points ($\varphi_T = 0.374, 0.432$) are illustrated by the distribution in the vector form of the velocity components, which represent departures from the designed axially symmetrical potential flow field. The secondary velocity is the result of W_r, the radial component, and W_ϑ, the circumferential velocity component. In the wake area, for the operating point ($\varphi_T = 0.432$) imbalance between centrifugal and pressure forces results in the radial velocity

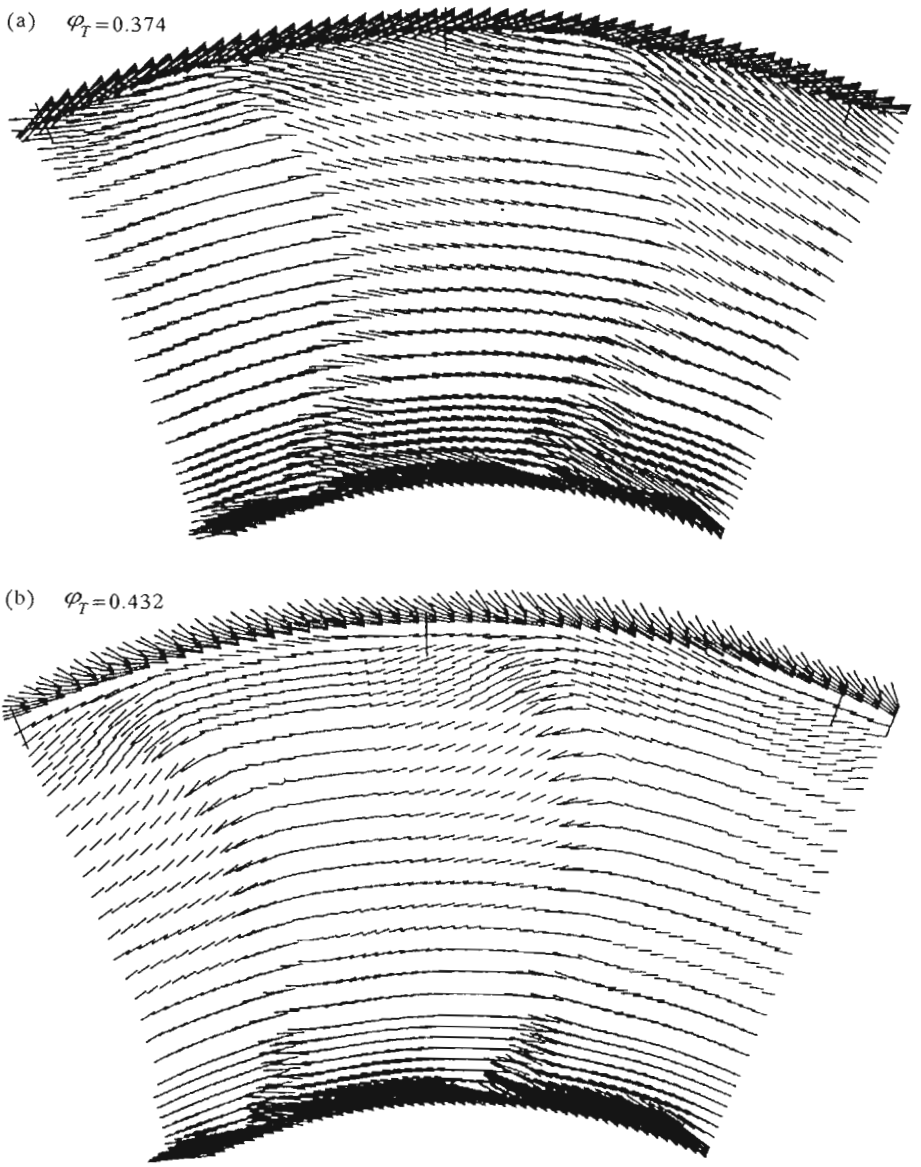

Fig. 11. Secondary flow field in the absolute system downstream of the rotor for two operating points

component being directed inward at midspan and upward at the hub and at the outer wall. But for the normal compressor operation (φ_T = 0.374) the inward-directed radial flow occurs only in the area close to the tip of the blade impeller suction side as a result of the leakage flows. It is clearly visible on the larger plot of the secondary velocity vectors close to the tip clearance gap (Fig.12).

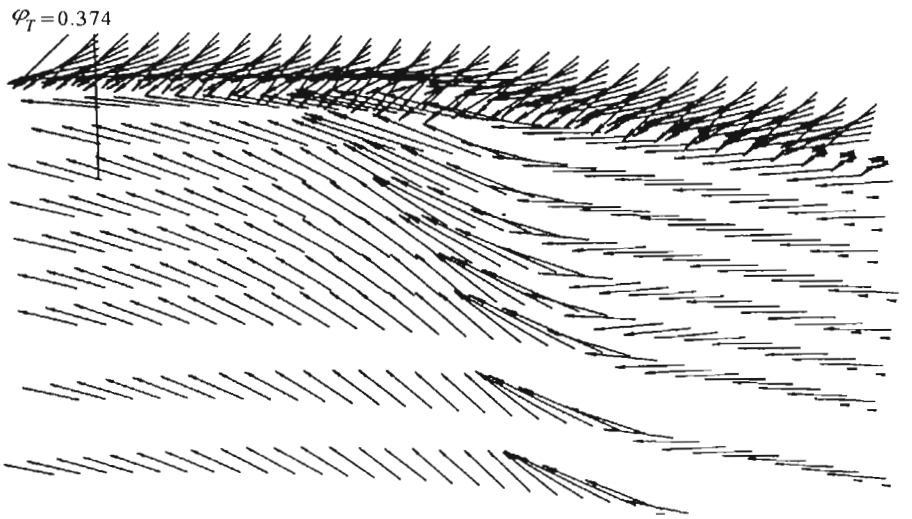

Fig. 12. Velocity vectors showing tip leakage effects

11. Conclusions

- The work presented here represents only a preliminary study in which measurements have been taken for two flow coefficients only.
- The results of experiments show that the triple-split fiber probes straight and 90° measurements combined with the ensemble average technique constitute a very useful method for the analysis of rotor flow in turbomachinery.

From the experimental results reported in this paper the following detail conclusions can be drawn:

- The axial and tangential components of turbulence structure at the midspan are nearly symmetrical about the wake centerline behind the rotor blade under both operation conditions. The radial components are strongly asymmetrical. It results from the imbalance between centrifugal and pressure forces in the wake area.

- The turbulence structure of the wake in location 3, for the middle radius, at both flow coefficients accounts for nearly isotropic turbulence outside the wake and anisotropic turbulence in the wake region. The axial and radial turbulence intensity in the rotor blade wake are smaller then the circumferential ones. The maximum axial turbulence at the midspan in the rotor wake reach values about 11 percent, whereas tangential values reach about 27 percent.

- Far downstream the rotor wake decrease significantly so it does not influence the incidence of the downstream stator. That method makes possible to find the proper axial distance between the rotor and stator blade rows.

- The strong backward reaction of the stator blade inlet edges to the tangential turbulence intensities and turbulence correlations, at a higher value of flow rate, have been found. It is probably caused by off-design incidence of the stator at the off-design point of operation.

- The highest velocity fluctuations, Reynolds stresses and turbulence intensity, respectively, are detected in the hub and tip regions. In contrast to the results for the maximum value of the flow coefficient, the axial component of turbulence is found to be the lowest and tangential component to be the largest in the leakage flow mixing region, at the nominal flow coefficient. High values of tangential intensities at this point of operation may be due to the fact of higher magnitude of aerodynamic load, providing an increase in leakage flow.

- If the turbulence production at the rotor exit is compared for the normal and higher values of flow rate, significant differences occur only in the tip region of the rotor blade.

- The issue of understanding the flow effects depending on the operation point and particularly those appearing near the stability line of a comporessor is of crucial interest for understanding of flow effects near the stall line. Hönen and Gallus (1993) demonstrated that the rotor outlet unsteady flow field changed more significantly as the operating point of

the compressor approached the stability line. The prediction of the stability limit by means of such a method is practically feasible and should be solved in the nearest future.

References

1. BENDAT I.S., AND PIERSOL A.G., 1986, *Random Data Analysis and Measurement Procedures*, Wiley, New York, 425-483

2. BINDER A., SCHROEDER TH., HOURMOUZIADIS J., 1989, Turbulence Measurements in a Multistage Low-Pressure Turbine, *ASME Journal of Turbomachinery*, **111**, 153-161

3. DAVINO R., LAKSHMINARAYANA B., 1982, Turbulence Characteristics in the Annulus-Wall Boundary Layer and Wake Mixing Region of a Compressor Rotor Exit, *ASME Journal of Engineering for Power*, **104**, 561-570

4. GALLUS A.E., POENSGEN C., ZESCHKY J., 1991, A Comparison between the Unsteady Flow Field in an Axial Flow Compressor and an Axial Flow Turbine, *European Propulsion Forum*, Paris, 1-19

5. HANSON H.P., 1983, Measurements of Wake Generated Unsteadines in the Rotor Passages of Axial Flow Turbines, *Journal of Enginering for Power*, **107**

6. HÖNEN H., AND GALLUS H.E., 1995, Monitoring of Aerodynamic Load and Detection of Stall in Multistage Axial Compressors, *ASME Journal of Turbomachinery*, **117**, 81-86

7. JØRGENSEN F.E., 1982, Characteristics and Calibration of a Triple-Split Probe for Reversing Flows, *DISA Information*, 27

8. LAKHSMINARAYANA B., AND PONCET A., 1974, A Method of Measuring Three Dimensional Rotating Wakes Behind Turbomachinery Rotors, *ASME Journal of Fluids Engineering*, **96**, 871-916

9. SCHULTZ H.D., 1989, Experimentalle Untersuchung der Dreidimensionalen abgelösten Strömung in einem Axialverdichterringgitter, Dissertation, Aachen 1989

10. WITKOWSKI A., CHMIELNIAK T., STROZIK M., MIRSKI M., 1993, Metoda pomiaru turbulencji i zjawisk nieustalonych w stopniu wentylatora osiowego, *Zeszyty Naukowe Pol. Śląskiej*, **118**

11. WITKOWSKI A., CHMIELNIAK T., STROZIK M., MIRSKI M., 1994a, Stand for Investigations of Threedimensional Turbulent Flow in Axial Compressing Stage. *The Archive of Mechanical Engineering*, **XLI**, 3-4

12. WITKOWSKI A.S., CHMIELNIAK T.J., STROZIK M.D., 1996, Experimental Study of a 3D Wake Decay and Secondary Flows behind a Rotor Blade Row of a Low Speed Compressor Stage, *ASME 96-GT-415*, New York

Identyfikacja śladu pozałopatkowego oraz trójwymiarowej struktury turbulencji w osiowym, niskoobrotowym stopniu sprężającym

Streszczenie

Przedstawiono wyniki badań struktury turbulencji w obszarze śladu pozałopatkowego niskoobrotowego koła wirnikowego sprężarki osiowej. Badania przepływu nieustalonego przeprowadzone zostały w dwóch punktach charakterystyki aerodynamicznej, przy zastosowaniu cyklicznego, zsynchronizowanego z kątowym położeniem koła wirnikowego systemu pomiarowego z wykorzystaniem prostej i kątowej wersji sondy termoanemometrycznej, z trójdzielną folią, w celu określenia wpływu obciążenia aerodynamicznego na charakter przepływu turbulentnego. Zastosowana metoda badawcza umożliwia rozpoznanie zjawisk występujących w obszarze szczeliny nadłopatkowej, przepływów wtórnych, intensywności turbulencji, naprężeń Reynoldsowskich oraz obserwację zanikania śladu pozałopatkowego koła wirnikowego w szczelinie międzywieńcowej stopnia sprężającego.

Manuscript received October 10, 1996; accepted for print January 22, 1997